ICES C.M. 1995

C.M. 1995/Q:26

Theme Session on "'Intermediate-Scale Physical Processes and
Their Influence on the Transport and Food Environment of Fish"
1995 ICES Annual Science Conference
21-26 September 1995, Åalborg, DENMARK

LARVAL TROPHODYNAMICS, TURBULENCE, AND DRIFT ON GEORGES BANK: A SENSITIVITY ANALYSIS OF COD AND HADDOCK

Francisco E. Werner[1], R. Ian Perry[2], Brian R. MacKenzie[3],
R. Gregory Lough[4] and Christopher E. Naimie[5]

[1] Marine Sciences Program, University of North Carolina, Chapel Hill, NC, 27599-3300, USA
[2] Pacific Biological Station, Department of Fisheries and Oceans, Nanaimo, BC, V9R 5K6, CANADA
[3] Danish Institute for Fisheries & Marine Research, Charlottenlund Castle, DK-2920 Charlottenlund, DENMARK
[4] National Marine Fisheries Center, Northeast Fisheries Science Center, Woods Hole, MA 02543, USA
[5] Dartmouth College, Hanover, NH 03755, USA

Abstract

(ei Melanogrammus aeglefinus ed) (ei Gadus morhua)

Using a model-based approach we consider trophodynamic effects on the growth and survival of larval cod and haddock on Georges Bank during late winter/early spring. We examine: (i) larval search behavior and its effect on encounter with prey, (ii) the ability of larvae to pursue and capture prey in a turbulent environment, and (iii) the effect of turbulence on the dispersion of larvae in the vertical. These studies represent an extension of results described in Werner et al. (1995; *Deep-Sea Res. II*, in press.) wherein the effect of turbulence-enhanced larval-prey contact rates increased the effective prey concentration resulting in growth of cod larvae consistent with observed rates in the field. In the present study we find that search behavior, the effect of turbulence on pursuit and capture, and vertical dispersion, decrease the predicted larval growth rates. These results suggest that larval feeding behavior, and especially the ability of larvae to pursue encountered prey, could be an important input to larval growth and survival models. Until larval feeding behavior in turbulent environments is better described, interpretations of how turbulence affects ingestion and growth rates in populations of larval cod and haddock should be regarded as preliminary. The inclusion of turbulence in determining the position of passive larvae in the water column allows the larvae to sample the entire water column contributing to a decrease in the variance of the size of the larvae over time. The ability of larvae to swim and aggregate in the vertical will be necessary to reproduce distributions observed in the field.

1 Introduction

Spatially explicit individual-based models of larval fish trophodynamics can be used to explore the relative importance of biological and physical variables on larval growth and survival. Conceptually, a greater contribution to the recruiting population may be made by larvae in poor growth areas if these areas also have longer retention time-scales, compared with larvae in areas of good growth but which experience high advective through-flows. The problem is to determine

the relative magnitudes of growth rates and retention time-scales. Our studies of larval cod and haddock on Georges Bank have shown that predicted survival and growth rates for cod larvae are comparable to those observed in the field for larvae that are located below the pycnocline where the turbulence-enhanced contact rates are greatest (Werner et al. 1995). In contrast, the findings for larval haddock indicate lower growth rates than those observed on the Bank, suggesting that haddock larvae require higher prey concentrations.

In the present study we use our modeling approach to examine the sensitivity of larval cod and haddock growth and survival to alternate representations of the larval feeding environment on Georges Bank. First, we consider the effect of the inclusion of larval behavior in the determination of larval-prey contact rates. Second, we examine the effects of turbulence on post-encounter behaviors (capture and ingestion success), and third, we include the effects of the turbulent dispersion on the vertical position of the larvae.

Our long-term objective is to identify realistic combinations of the circulation components and prey-field structures that can reproduce the observed range of growth and survival rates, and to evaluate the relative sensitivity of cod and haddock larvae to aggregated prey distributions and spatially and temporally heterogeneous (turbulent) flow fields.

2 Prey Field

Representative concentrations of zooplankton prey and their distributions on Georges Bank, for the February-April time-period were determined from the literature and assumptions detailed in Werner et al. (1995). Briefly, Kane (1984) identified the various life history stages of *Pseudocalanus minutus, Calanus finmarchicus, Oithona similis*, and *Centropages* sp. as the dominant components of the diets of larval cod and haddock on Georges Bank. Our specification of the prey field concentrates on these four taxonomic groups. Georges Bank was separated into northern flank (NF), eastern flank (EF), southern flank (SF) and central cap (CC; depths less than 40 m) regions (Figure 1) based on Davis (1984).

Table 1 summarizes the larval fish prey sizes and weights, and the assigned concentrations within each of the four regions on Georges Bank for late-winter/early spring. These distributions were prescribed as time-invariant and vertically uniform within each region. Although we recognize this is an artificial constraint, it is justified as a first simplifying assumption consistent with the relatively little difference in regional abundances of major prey items and the absence of persistent vertical stratification between February and March-April. Additionally, we assumed that larval fish feeding had no impact on prey abundance or distribution (e.g., Cushing 1983).

Using the Table 1 prey field estimates Werner et al. (1995) found that cod and haddock larvae will starve on Georges Bank. Five-fold increases in the mean prey concentrations were necessary for cod larvae to survive, while fifteen-fold increases were required for survival of haddock larvae. However, the inclusion of spatially-variable and time-dependent turbulence generated by winds and tides was found to increase prey contact rates two- to five-fold, effectively increasing the prey concentration perceived by the larvae. The result was an increase in the larval growth and survival rates that are comparable with observed growth rates for those larvae located below the surface layer (deeper than 25 m) and inside the 60 m isobath where tidally-induced turbulence

Table 1: Egg and zooplankton prey type, mean size (length), mean weight (dry weight) of each size class, and assigned concentrations within each of the four regions on Georges Bank (northern flank, eastern flank, southern flank, central cap).

Prey Type	Size (mm)	Weight (μgDW)	N. Flank #/liter	E. Flank #/liter	S. Flank #/liter	C. Cap #/liter
Eggs	<0.13	1.60	2.14	2.14	2.14	2.14
Nauplii	0.28	1.20	1.08	12.30	6.36	12.78
C-I	0.42	1.10	0.05	0.49	0.22	0.62
C-II	0.52	1.82	0.05	0.32	0.24	0.35
C-III	0.62	2.89	0.02	0.08	0.22	0.12
C-IV	0.73	4.80	0.04	0.08	0.27	0.11
C-V	0.88	9.58	0.04	0.07	0.31	0.11
C-VI	>0.88	16.67	0.18	0.11	0.24	0.06

in the bottom boundary layer provides the required increases in prey contact rates. Thus, the region of highest retention due to circulation processes (Werner et al. 1993; Lough et al. 1994) coincides with the region of highest growth rates: shoalward of the 60 m isobath, at subsurface depths of 25 m or greater. Despite the enhanced contact rates due to turbulence, haddock larvae required higher prey densities (by a factor of five) than cod larvae to survive.

In the present study, we use two prey field estimates: that in Table 1 and another in which the concentration of the four smallest prey items (eggs, nauplii and C-I and C-II copepodite stages) are increased four-fold. In nature, plankton are patchily distributed at small spatial scales. For example, in both calm and turbulent conditions off Peru and California, Owen (1989) found patches of plankton at scales of 0.2-2 m, and plankton abundance within the patches was typically 2-4 times greater than outside the patches. In addition, Davis et al. (1992) found patches of copepods at scales of 20-30 cm in nearshore waters off Massachusetts. On Georges Bank the distribution of plankton at such small scales is currently under study, but given the presence of small-intermediate scale patchiness in other systems (e.g., Jenkins 1989) we expect that plankton on the Bank will be patchily distributed at similar spatial scales. Since this scale of patchiness is not recorded by towed zooplankton nets, our prey concentrations may be low. To allow for this possibility, we increased four-fold the concentration of the four smallest prey classes in some of the studies below. We indicate this by the factor F_f=4:1 versus F_f=1:1 in the discussion that follow.

3 Physical Model Flow Field

The three-dimensional, nonlinear, prognostic (evolving baroclinic field), finite element hydrodynamic model employed is that of Lynch et al. (1995). The model operates in tidal time and uses the quasi-equilibrium version of Mellor-Yamada level 2.5 turbulence closure scheme (Mellor

and Yamada 1982; Galperin et al. 1988), by including the turbulent kinetic energy ($q^2/2$) and mixing length (l) as hydrodynamic state variables that are functions of position and time.

The circulation field we use in this study corresponds to climatological March-April conditions, consistent with the spawning and early larval drift period of cod and haddock on Georges Bank. Initial conditions are based on the M_2 tide and the mean circulation, density, and wind fields described by Naimie et al. (1994) for the March-April bimonthly period. The computation includes boundary forcing from the M_2 tide and surface forcing from the mean wind stress (0.0472 Pa toward 121.4 degrees clockwise from true North). At the open boundaries the low-frequency and the M_2 forcings are specified, and the vertical structure of density is fixed at the climatological conditions (see Naimie 1995a and 1995b). The depth-averaged flow field is shown in Figure (2) and shows the familiar clockwise pattern around Georges Bank, including the tidally rectified northern flank jet, the southwestward drift along the southern flank and the generally weak recirculation in the Great South Channel during this season. A snapshot of the Bank-wide depth-averaged turbulent kinetic energy dissipation rate $\bar{\epsilon}$ (W/Kg), a vertical section of ϵ across the Bank and a time-series at a station inside the 60 m isobath are shown in Figure (3). These results are in good agreement with Loder et al. (1993) and Horne et al. (1995).

For purposes of larval advection (i.e., particle tracking) and trophodynamic calculations we retained only the residual, the M_2 and M_4 components of velocity and relevant turbulent quantities; those components of velocity and turbulence at the M_6 frequency found not to significantly affect our results. The effect of the wind is included in the mean circulation and turbulence components. The particle (larval) positions 20, 40 and 60 days post-spawn are shown in Figure (4) for two cases: non-turbulent (as in Werner et al. 1995) and turbulent dispersal of larvae in the vertical (see Section 7 herein). Spawning is assumed to occur on the Northeast Peak, and the larvae drift passively with the circulation. Particles were released over the Northeast Peak at 1, 10, 20, 30, 40 and 50m in a square region 62.5 Km on a side (Figure 1). At each horizontal level there were 121 particles equally spaced in an 11x11 grid, resulting in a total of 726 particles per release. The egg-phase is assumed to be 20 days long (Page and Frank, 1989). At 20 days post-spawn the larvae hatch and trophodynamic processes (feeding, growth, starvation) begin. We consider trophodynamics only for the first 40 days of the larval period for a total length of the simulations of 60 days: a 20-day egg-phase and a 40-day larval-phase.

4 Trophodynamic Model

The core of our model (Werner et al. 1995) is the standard bioenergetic supply-demand function, in which growth is represented as the difference between the amount of food absorbed by a larva and the metabolic costs of its daily activities. Beyer and Laurence (1980 and 1981) used this approach in individual-based models of winter flounder and Atlantic herring larvae. The amount of food ingested is a function of such processes as the number of prey encountered, captured and eaten, while the metabolic costs are a function of larval size, ambient temperature, swimming speed, etc. Larvae are assumed to die (of starvation) if their weight falls below a prescribed "death barrier". Using relationships derived from laboratory studies on the physiology and growth of Atlantic cod and haddock eggs and larvae, Laurence (1985) presented a model which included individual variation in hatch-size, prey density, prey size, and prey encounter rate. Our

trophodynamic model is an elaboration of Laurence's (1985) model. In Laurence's formulation, ingestion of a single preferred prey size is modeled. In our model, the prey biomass ingested by the larvae is a combination of the eight specified prey categories, with proportions of the ingested prey categories determined by Kane's (1984) analysis of the gut contents of particular size categories of cod and haddock larvae.

The individual based modeling (IBM) approach used here, is a natural extension of Lagrangian particle-tracking descriptions of the circulation, and provides a useful tool in the study of the variability in feeding and growth characteristics of individual larvae. The approach integrates the unique temporal and spatial history of the individual larvae, each of which is exposed to different prey concentrations and physical parameters. In this manner, the growth of individual larvae can be understood in terms of a detailed time-history of the food available to the larva, which itself is a function of the unique trajectory of each larva through the prey field, and the ability to encounter (and capture) the prey.

5 Effect of Turbulence on Encounter Rates

5.1 Cruise searching behavior

Rothschild and Osborn (1988) discussed the role of turbulence in affecting (enhancing) encounter rates with planktonic prey. Subsequent studies, e.g., Sundby and Fossum (1990), MacKenzie and Leggett (1991), Muelbert et al. (1994) and Werner et al. (1995), explored the role of turbulence in oceanic conditions, finding an effective increase in contact rates of 2-10 under various wind- and tidally-driven flows. With this formulation, we estimate $N(i)$ the number of ith prey of concentration $p(i)$ encountered over a 24-hour period in a turbulent environment from

$$N(i) = \sum_{24\,\mathrm{h}} \mathcal{L} \cdot A(i) \cdot D(i) \cdot p(i) \cdot \Delta t \tag{1}$$

with a time step Δt of 1 hour. The effect of the turbulent velocity ω enters in the determination of $A(i)$, the velocity of a larval fish relative to its prey

$$A(i) = \frac{[\sigma^2_{\mathrm{prey}}(i) + 3\tau^2 + 4\omega^2]}{3(\tau^2 + \omega^2)^{1/2}} \tag{2}$$

where the larval fish swimming speed τ, and the ith prey swimming speed $\sigma_{\mathrm{prey}}(i)$ are assumed here as one body-length per second. In Eq. (1) $\mathcal{L}$ is a binary day/night switch and $D(i) = (2/3)\pi\rho^2$ is the cross-sectional area of perception of the larva, where $\rho = (3/4)L_{c,h}$ is the prey encounter radius and is related to $L_{c,h}$ the larval cod or haddock body length (Laurence, 1978).

The turbulent velocity (squared) is

$$\omega^2 = 3.615(\epsilon\tau)^{2/3} \tag{3}$$

where the separation distance can be approximated (Rothschild, 1992) as

$$r = 0.55p(i)^{-1/3} \tag{4}$$

a.l $\epsilon = q^3/(B_1 l)$ is the rate of turbulent kinetic energy dissipation obtained at every point in s ace and time throughout the model domain. The turbulent velocity q and the mixing length l are obtained from the circulation model and $B_1(= 16.6)$ is a constant (Mellor and Yamada, 82; Galperin et al. 1988). In Figure (5) we show the survival and growth time-history for the se of cruise search behavior with F_f=4:1. The survival and growth time-history for the case f cruise search behavior and F_f=1:1 is described in Werner et al. (1995) and summarized in Table 2 (compare Cases 1 and 5).

5.2 Pause-travel searching behavior

Considering that cod larvae are pause-travel predators, and that the spatial scale during encounter is defined by larval reactive distance, MacKenzie and Kiørboe (1995) formulate an expression for the encounters (# prey/sec) as

$$E_{\mathrm{p-t}}(i) = \frac{2}{3}\pi R^3 p(i) P_F + \pi R^2 p(i)(\tau^2 + 2\omega^2)^{0.5} P_F P_D \tag{5}$$

where R is the larval reactive distance (taken here as 0.8×body-length of the larva), P_F is the pause frequency (#/sec), P_D is the pause duration (sec), and $p(i)$ and τ are as above. Note that when implementing Eq. (5) the computation of ω [Eq. (3)] is based on the larval reactive distance R instead of the mean predator-prey separation distance [Eq. (4)]. Finally, we modify Eq. (1) to include estimates of encounters based on Eq. (5)

$$N(i) = \sum_{24\,\mathrm{h}} \mathcal{L} \cdot E_{\mathrm{p-t}}(i) \cdot \Delta t \tag{6}$$

Figure (6) shows the survival and growth time-history for the case of pause-travel behavior with F_f=4:1. The survival and growth time-history for the case of cruise search behavior and F_f=1:1 is summarized in Table 2 (compare Cases 2 and 6).

6 Effect of Turbulence on Pursuit Success

A model for the influence of small-scale turbulence on post-encounter processes in larval fish finds that turbulence can have an overall beneficial or detrimental effect on larval fish ingestion depending on the magnitude of the turbulence and on larval behavior (MacKenzie et al. 1994). A dome-shaped relationship is found where ingestion rates are maximal at intermediate rather than high levels of turbulence; the reduction in pursuit success in highly turbulent environments negates the increase in ingestion rate caused by the increase in encounter rate. The implementation of this formulation is achieved by scaling the number of prey encountered [either Eq. (1) or Eq. (6)] by the estimated probability of successful pursuit P_{sp}.

Table 2: Summary of number of live cod or haddock (c/h) larvae on Georges Bank at day 40, their mean weight (μg) at day 40, and their mean relative depth ($\bar{z}_r$=depth of larvae/local depth; $\bar{z}_r \rightarrow 0$ near surface, $\bar{z}_r \rightarrow 1$ near bottom) for cases with nomenclature as follows: C=cruise behavior, P-T=pause-travel behavior, F_f=1:1 (mean prey concentration as in Table 1), F_f=4:1 (four-fold increase of four smallest prey categories), P_{sp} with time of pursuit t_p=1.7 sec, P_{sp} with time of pursuit t_p= 1.0 sec, M=Markov based turbulent vertical dispersion. A case where a condition does not apply is indicated by (n.a.); cases where there are no survivors are indicated by (-). Bolz and Lough (1988) measured mean weights of 40 day old cod larvae of 2466 μg, and of 4160 μg for 40 day old haddock.

Case #	Larval Behavior	F_f	P_{sp} t_p (s)	M	Day 40 % alive	Day 40 mean μg	Day 40 $\bar{z}_r$
1	C (c/h)	1:1	n.a.	n.a.	2.2/-	374/-	0.96/-
2	P-T (c/h)	1:1	n.a.	n.a.	0.7/-	221/-	0.98/-
3	C (c/h)	1:1	1.7	n.a.	-/-	-/-	-/-
4	P-T (c/h)	1:1	1.7	n.a.	-/-	-/-	-/-
5	C (c/h)	4:1	n.a.	n.a.	73.3/3.0	2802/1715	0.49/0.90
6	P-T (c/h)	4:1	n.a.	n.a.	57.7/1.1	2691/1768	0.51/0.98
7	P-T (c/h)	4:1	1.7	n.a.	1.9/-	50/-	0.16/-
8	P-T (c/h)	4:1	1.0	n.a.	44.8/-	416/-	0.49/-
9	P-T (c/h)	4:1	1.0	yes	62.6/-	276/-	0.48/-

The value of P_{sp} depends on the turbulent velocity ω, the pursuit time t_p and the larval reactive distance R. The intersection of the prey excursion sphere (of radius ωt_p) and the larval encounter sphere (of radius R) define appropriate values of P_{sp} (MacKenzie et al. 1994). If the radius of the prey's excursion sphere is less than the radius of the larval encounter sphere, $\omega t_p < R$,

$$P_{sp} = a_0\Big\{a_1 + a_2\Big[\ln R - \ln(R - \omega t_p)\Big]\Big\} \tag{7}$$

whereas, if the radius of the prey's excursion sphere is greater than or equal to the radius but less than the diameter of the larval encounter sphere, $R \leq \omega t_p < 2R$,

$$P_{sp} = a_0\Big\{a_1 + a_2\Big[\ln R - \ln(\omega t_p - R)\Big]\Big\} \tag{8}$$

or finally, if the radius of the prey's excursion sphere is greater than or equal to the diameter of the larval encounter sphere, $2R \leq \omega t_p$,

$$P_{sp} = \frac{R^3}{(\omega t_p)^3} \tag{9}$$

where $a_0 = 1/[64R(\omega t_p)^3]$, $a_1 = 44R(\omega t_p)^3 - 21(\omega t_p)^4 + 6R^2(\omega t_p)^2 + 12R^3\omega t_p$, and $a_2 = 24R^2(\omega t_p)^2 - 12R^4 - 12(\omega t_p)^4$.

The survival and growth time-history for the case of pause-travel behavior with F_f=4:1 and including the effect of turbulence on the ability of larvae to pursue and capture encountered prey are shown in Figure 7 (pursuit time t_p=1.7 sec; Case 7 in Table 2) and Figure 8 (pursuit time t_p=1.0 sec; Case 8 in Table 2). Note that if F_f=1:1 (Cases 3 and 4 in Table 2) no larvae survive.

7 Effect of Turbulence on Larval Dispersion

In previous studies (Werner et al. 1993 and 1995) we did not consider the effect of random, turbulent "kicks" that modify the larval vertical distributions. We follow the approach described by Legg and Raupach (1982) wherein the Langevin equation is used to derive a Markov equation for the vertical velocity of a particle (or larva) in a flow where the turbulence is inhomogeneous. The Langevin equation for the dispersion of particles is

$$\frac{\mathrm{d}w}{\mathrm{d}t} = -\alpha w + \lambda\xi(t) + F \tag{10}$$

where $\alpha = 1/\tau_l$ and τ_l is the Lagrangian integral time scale (or auto-correlation time scale) estimated from $N_q = \sigma_w^2\tau_l$, where N_q is the turbulent exchange coefficient (see Galperin et al. 1988), $\sigma_w(= 0.3q^2/2)$ is the Lagrangian velocity variance; $\lambda = \sigma_w\sqrt{2/\tau_l}$; $\xi(t)$ is Gaussian noise of

zero mean and unit variance; and $F = \partial(\sigma_w^2)/\partial z$ is a term involving the gradient in the turbulent velocity variance.

The Markov chain for w_{n+1}, the turbulent vertical velocity at time step $n+1$, becomes

$$w_{n+1} = a_n w_n + b_n \sigma_{wn} \xi_n + C_n \tag{11}$$

where $a_n = \exp(-\Delta t/\tau_{l_n})$, $b_n = [1 - \exp(-2\Delta t/\tau_{l_n})]^{1/2}$ and $C_n = (F/\alpha)[1 - \exp(-\Delta t/\tau_{l_n})]$, and Δt=1 minute was used. The values of τ_l were of the order of 250 to 300 sec (with a standard deviation of $\pm$150 sec), with turbulent velocity kicks of $\pm$1 cm/s (within a standard deviation of zero) implying turbulent vertical eddy motions of 1.5 to 4 meters.

The dispersal of particles in inhomogeneous turbulent fields can lead to aggregations that are not realistic if the dispersal process is not treated in the above manner (e.g., Legg and Raupach, 1982; Thomson, 1987; and Holloway 1994). One of the criteria that must be met is that an initially uniform distribution of particles must remain uniformly distributed over time, e.g., spatial non-uniformities of turbulence intensity cannot "un-mix" an initially well mixed situation. Even in a stratified case, i.e., in the presence of a pycnocline, if there is an initially well mixed distribution of particles (larvae), they should remain well mixed over time. However, those particles that are initially in the upper/lower layer will sample mainly the upper/lower layer and remain well mixed in the upper/lower layer. Those particles that are initially in the pycnocline, where the turbulence is decreased versus the upper and lower layers, will remain in the pycnocline region for longer periods, albeit with the a finite probability of being "kicked out" of the pycnocline, and with a finite probability that a particle (larva) from the upper and/or lower layer will be "kicked" into the pycnocline. Hence, some particles in this stratified case, initially in the upper/lower layer, will make it across the pycnocline to the lower/upper layer. In the end, the net flux of (passive, neutrally buoyant) particles through any depth level should be (close to) zero resulting in no net accumulation (un-mixing) of particles.

In the present set of simulations, the inclusion of F, the gradient in the turbulent velocity variance, is critical. If this term is ignored, particles (larvae) that are released unformly over depth are "kicked out" of the bottom layer (where tidal turbulence is strongest) and unrealistically accumulate in the surface layers of the water column. Comparison of the trajectories of a particular larva (without turbulent kicks, with turbulent kicks, and with turbulent kicks computed without the term F) is shown in Figure 9; the mean depth over the 40-day larval period was $-$38m for the non-turbulent trajectory, $-$23m for the turbulent trajectory without the gradient in the turbulent velocity variance (F), and $-$36m for the turbulent trajectory computed using Eq. (10). The survival and growth time-history for the case of pause-travel behavior with F_f=4:1, including the effect of turbulence on the ability of larvae to pursue and capture encountered prey (with pursuit time t_p=1.0 sec), and including the effect of turbulent kicks on the computed larval trajectories is shown in Figure (10) and summarized in Table 2 (Case 9).

8 Discussion

The model studies presented here allowed us to consider certain effects of larval cod and haddock search behavior and their encounter with prey, the effect of turbulence on the ability of larvae to pursue and capture prey, and the effect of turbulence on the dispersion of larvae in the vertical. One set of simulations compared the effects of using different assumptions regarding larval search behavior and the appropriate spatial scale for calculating turbulent velocities. Most earlier estimates of larval fish encounter rates assumed that larvae were cruise searchers instead of pause-travel searchers (e.g., Sundby and Fossum 1990, Davis et al. 1991, MacKenzie and Leggett 1991). In cruise search strategies, the spatial scale to be used in calculating relative particle velocities is much larger (e.g., average distance between prey particles, size of eddies; Sundby and Fossum 1990, Davis et al. 1991, MacKenzie and Leggett 1991, Muelbert et al. 1994, Werner et al. 1995) than that for pause-travel search strategies (i.e., the larval reactive distance; Evans 1989; Denman and Gargett 1995). Our results using both sets of assumptions show that when cod larvae are treated (correctly) as a pause-travel predator with the spatial scale during encounter defined by larval reactive distance, their expected growth and survival rates are lower than if considered (incorrectly) as a cruise predator with spatial scale defined by mean distance between prey particles (Figs. 5 and 6; also Table 2 Cases 1 and 2; 5 and 6).

A second set of simulations addressed how turbulence might affect the ability of larvae to pursue and capture prey once they are encountered. These simulations showed that larvae would not survive on Georges Bank using the food concentrations typically measured with large-scale plankton samplers, and assuming that the larval diet consists of copepod nauplii and copepodites (Table 2, Cases 3 and 4). Since this observation contradicts the field results, it suggests that inputs to the model may not be realistic representations of the larval feeding environment or larval behavior. To address this possibility, we conducted a sensitivity analysis of our model.

Using the higher prey concentration, and allowing for turbulence-dependent pursuit success (MacKenzie et al. 1994), with larval pursuit times t_p=1.7 sec, resulted in a larval survival rate of 2% for cod, and growth rates barely above the Death Barrier (Fig. 7), which is well below that observed in the field (Bolz and Lough, 1988). In addition, survivors were concentrated in the upper half of the water column (Fig. 7; also Table 2) rather than the bottom boundary layer as found by Werner et al. (1995). This distribution is due to the low-moderate levels of turbulence in the upper layer (Fig. 3), which have positive effects on encounter, but negligible effects on pursuit success.

These simulations suggest that understanding the processes affecting growth and survival of cod and haddock larvae on Georges Bank requires a better description of the *in situ* feeding environment at small to intermediate scales (<50-100 m), and how prey patchiness is affected by turbulence. Unfortunately, the ability of cod and haddock larvae to locate and remain associated with such patches is not known, although field sampling on Georges Bank shows that haddock and cod larvae have aggregated vertical distributions (Buckley and Lough 1987). Interestingly, other species of fish larvae (e.g., anchovy, herring) alter their swimming behavior after encountering a prey patch in order to increase the probability of remaining within the patch (Hunter and Thomas 1974, Munk and Kiørboe 1985). It is possible therefore that cod and haddock larvae may be able to feed at rates higher than we have calculated in the prey density simulations

considered herein.

The other input to the feeding model which we varied was the time required for larvae to successfully pursue an encountered prey item. This input defines the amount of time that larvae require to pursue and capture a prey particle as it is being advected through the larva's visual field. Pursuit times for small cod larvae in calm water are about t_p=1.7 sec (H. Browman, pers. comm., cited in MacKenzie et al. 1994). However, if larvae react more rapidly to encountered prey items (i.e., t_p=1 sec), our simulations show that predicted survival and growth rates are considerably higher than in the slower pursuit case (Fig. 8; Table 2, Cases 7 and 8).

These results suggest that larval feeding behavior, and especially the ability of larvae to pursue encountered prey, should be an important input to larval growth and survival models. For example, Kiørboe and Saiz (1995) have modified the original MacKenzie et al. (1994) pursuit model to allow the turbulent velocity ω to decrease during pursuit. This modification results higher pursuit success than that in our calculations. Unfortunately, present descriptions of larval pursuit success in turbulent water require an extrapolation of pursuit behaviors observed in calm water. This extrapolation is necessary because descriptions of larval fish feeding behavior in turbulent conditions are presently unavailable. In addition, and due to the lack of data, our simulations further assume that pursuit time is independent of larval size, larval species (cod vs. haddock), and prey behavior. Hence, until larval feeding behavior in turbulent situations is better described, interpretations of how turbulence affects ingestion and growth rates in populations of larval cod and haddock should be regarded as preliminary steps towards a complete understanding of interactions between larvae and their prey.

A third set of simulations considered the effect of larval dispersal in the water column due to random/turbulent motions. Our results (Figs. 9 and 10) suggest that turbulence allows passive (non-swimming, non-buoyant) larvae to sample the entire water column several times over a 40-day period. In othe words, larvae that were released in the top (bottom) layers will, through turbulent kicks, be "bumped" to the bottom (top), then back to the top (bottom), etc. The standard deviation of the turbulent velocities that larvae encounter is on the order of $\pm$1 cm/s, and hence a larva that is 5-7 mm in length, swimming at a body-length per second should be able to sustain its position or even overcome the turbulent "kick". In our case, sampling the entire vertical region results is a reduction in the variance of the larval sizes at the end of 40 days. For example, the mean length of the larvae at day 40 in Figure (8) is 8.1 mm ($\pm$ 1.6 mm) and that in Figure (10) is 7.9 mm ($\pm$ 1.0 mm) [or in terms of dry weight 329μg ($\pm$ 0.4) for Figure (8) and 294μg ($\pm$ 0.06) for Figure (10)]. This is as expected, since rather than some larvae always being in regions favorable for growth and some always in less favorable regions, all larvae will sample all regions, resulting in a population of "average" larvae with reduced variance in size. Previous studies have described the general two-layer circulation of Georges Bank and found that larvae located in the lower water column and near bottom have an increased probability of remaining on the Bank (e.g., Werner et al. 1993). However, including this turbulent dispersion effect suggests that passive larvae will spend more time in the middle and upper water column where they may be at higher risk of advection off the Bank due to this two-layer circulation and occasional wind or storm events (e.g., Lough et al. 1994). The effect of behavior and the ability to aggregate (e.g., Lough 1984, Buckley and Lough 1987, Lough and Potter, 1993, Lough and Mountain, 1995) will be critical to model vertical distributions and subsequent horizontal

transports observed in the field.

Lastly, the time of the year we have considered is late winter early spring which is generally weakly stratified. The onset of stratification in late April/early June will result in suppression of turbulence in the vicinity of the pycnocline, and in a region where larvae and prey may actively aggregate and form patches due to behavior or buoyancy effects. These net increases in prey concentration (observed by Buckley and Lough 1987 and Incze et al. 1995) appear to be necessary to achieve observed growth rates of cod and (especially) haddock. Note that haddock were found to survive only in cases where prey concentrations were increased (F_f=4:1; Table 2, Cases 5 and 6) and the effects of turbulence on post-encounter capture, and vertical turbulent dispersion were not considered.

Acknowledgments

Discussions with D. Lynch, J. Loder, C. Hannah, F. Page, M. Sinclair and T. Gross were valuable in the preparation of this paper. We wish to thank B.O. Blanton for his help in various aspects of the particle tracking implementation and the preparation of the figures. This research was supported by the joint NSF-NOAA US GLOBEC Program and the Canadian Panel on Energy, Research and Development. BRM was supported by a grant from the European Union (AIR2 94 1226). A grant from NSF to J. Steele supported FW's travel to the ICES Meeting.

References

Beyer, J.E. and G.C. Laurence (1980) A stochastic model of larval growth. *Ecol. Modelling*, **8**, 109-132.

Beyer, J.E. and G.C. Laurence (1981) Aspects of stochasticity in modelling growth and survival of clupeoid fish larvae. *Rapp. P.-v. Reun. Cons. int. Explor. Mer*, **178**, 17-23.

Bolz, G.R. and R.G. Lough (1988) Growth through the first six months of Atlantic cod, *Gadus morhua*, and haddock, *Melanogrammus aeglefinus*, based on daily otolith increments. *Fish. Bull., U.S.*, **86**, 223-235.

Buckley, L.J. and R.G. Lough (1987) Recent growth, biochemical composition, and prey field of larval haddock (*Melanogrammus aeglefinus*) and Atlantic cod (*Gadus morhua*) on Georges Bank. *Can. J. Fish. Aquat. Sci.*, **44**, 14-25.

Cushing, D.H. (1983) Are fish larvae too dilute to affect the density of their food organisms? *J. Plankton Res.*, **6**, 591-599.

Davis, C.S. (1984) Interaction of a copepod population with the mean circulation on Georges Bank. *J. Mar. Res.*, **42**, 573-590.

Davis, C.S., G.R. Flierl, P.H. Wiebe, and P.J.S. Franks (1991) Micropatchiness, turbulence and recruitment in plankton. *J. Mar. Res.*, **49**, 109-151.

Denman, K.L. and A.E. Gargett (1995) Biological-physical interactions in the upper ocean: The role of vertical and small scale transport processes. *Ann. Rev. Fluid Mech.*, **27**, 225-255.

Evans, G.T. (1989) The encounter speed of moving predator and prey. *J. Plankton Res.*, **11**, 415-417.

Galperin, B., L.H. Kantha, S. Hassid, and A. Rosati (1988) A quasi-equilibrium turbulent energy model for geophysical flows. *J. Atmos. Sci.*, **45**, 55-62.

Holloway, G. (1994) Comment: on modeling vertical trajectories of phytoplankton in a mixed layer. *Deep-Sea Res.*, **41**, 957-959.

Horne, E.P.W., J.W. Loder and N.S. Oakey (1995) Turbulence dissipation rates and nitrate supply in the upper water column on Georges Bank. *Deep Sea Research II, Topical Studies in Oceanography*, in press.

Hunter, J.R. (1972) Swimming and feeding behavior of larval anchovy *Engraulis mordax. Fish. Bull.*, **70**, 821-834.

Incze, L.S., P. Aas, T. Ainaire (1995) Distribution of copepod nauplii and turbulence on the southern flank fo Georges Bank: implications for feeding by larval cod. *Deep Sea Research II, Topical Studies in Oceanography*, in press.

Jenkins, G.P. (1989). Micro- and fine-scale distribution of microplankton in the feeding environment of larval flounder. *Mar. Ecol. Prog. Ser.*, **43**, 233-244.

Jenkinson, I. and T. Wyatt (1992) Selection and control of Deborah numbers in plankton ecology. *J. Plankton Res.*, **14**, 1697-1721.

Kane, J. (1984) The feeding habits of co-occurring cod and haddock larvae. *Mar. Ecol. Prog. Ser.*, **16**, 9-20.

Kiørboe, T. and E. Saiz (1995) Planktivorous feeding in cal and turbulent environments, with emphasis on copepods. *Mar. Ecol. Prog. Ser.*, **122**, 135-145.

Laurence, G.C. (1978) Comparative growth, respiration and delayed feeding abilities of larval cod (*Gadus morhua*) and haddock (*Melanogrammus aeglefinus*) as influenced by temperature during laboratory studies. *Mar. Biol.*, **50**, 1-7.

Laurence, G.C. (1985) A report on the development of stochastic models of food limited growth and survival of cod and haddock larvae on Georges Bank, p. 83-150. In: G.C. Laurence and R.G. Lough (eds). Growth and survival of larval fishes in relation to the trophodynamics of Georges Bank cod and haddock. *NOAA Tech. Mem.*, **NMFS-F/NEC-36**, 83-150.

Legg, B.J. and M.R. Raupach (1982) Markov chain simulation of particle dispersion in inhomogeneous flows: The mean drift velocity induced by a gradient in Eulerian velocity variance. *Boundary-Layer Meteorol.*, **24**, 3-13.

Loder, J.W., K.F. Drinkwater, N.S. Oakey and E.P.W. Horne (1993) Circulation, hydrographic structure and mixing at tidal fronts: the view from Georges Bank. *Phil. Trans. R. Soc. Lond. A*, **343**, 447-460.

Lough, R.G. (1984) Larval fish trophodynamic studies on Georges Bank: sampling strategy and initial results. In: The propagation of cod *Gadus morhua L.*, E. Dahl, D.S. Danielssen, E. Moksness and P. Solemdal, eds. *Flodevigen rapportser*, **1**, 395-434.

Lough, R.G. and D.G. Mountain (1995) Effect of small-scale turbulence on feeding larval cod and haddock in stratified water on Georges Bank. *Deep Sea Research II, Topical Studies in Oceanography*, in press.

Lough, R.G. and D.C. Potter (1993) Vertical distribution patterns and diel migrations of larval and juvenile haddock *Melanogrammus aeglefinus* and Atlantic cod *Gadus morhua* on Georges Bank. *Fish. Bull. U.S.*, **91**, 281-303.

Lough, R.G., W.G. Smith, F.E. Werner, J.W. Loder, F.E. Page, C.G. Hannah, C.E. Naimie, R.I. Perry, M. Sinclair and D.R. Lynch (1994). Influence of wind-driven advection on interannual variability in cod egg and larval distributions on Georges Bank: 1982 vs 1985. *ICES mar. Sci. Symp.*, **198**, 356-378.

Lynch, D.R., J.T.C. Ip, C.E. Naimie and F.E. Werner (1995) Comprehensive coastal circulation model with application to the Gulf of Maine. *Continental Shelf Research*, in press.

MacKenzie, B.R. and T. Kiørboe (1995) Encounter rates and swimming behavior of pause-travel and cruise larval fish predators in calm and turbulent environments. *Limnol. Oceanogr.*, in press.

MacKenzie, B.R. and W.C. Leggett (1991) Quantifying the contribution of small-scale turbulence to the encounter rates between larval fish and their zooplankton prey: effects of wind and tide. *Mar. Ecol. Prog. Ser.*, **73**, 149-160.

MacKenzie, B.R., T.J. Miller, S. Cyr and W.C. Leggett (1994) Evidence for a dome-shaped relationship between turbulence and larval fish ingestion rates. *Limnol. Oceanogr.*, **39**, 1790-1799.

Mellor, G.L., and T. Yamada (1982) Development of a turbulence closure model for geophysical fluid problems. *Rev. of Geophys. Space Phys.*, **20**, 851-875.

Muelbert, J.H., M.R. Lewis and D.E. Kelley (1994) The importance of small-scale turbulence in the feeding of herring larvae. *J. Plankton Res.*, **16**, 927-944.

Munk,P. and T. Kiørboe (1985) Feeding behaviour and swimming activity of larval herring (*Clupea harengus*) in relation to density of copepod nauplii. *Mar. Ecol. Prog. Ser.*, **24**, 15-21.

Naimie, C.E., J.W. Loder and D.R. Lynch (1994) Seasonal variation of the three-dimensional residual circulation on Georges Bank. *J. Geophys. Res.*, **99**, 15,967-15,989.

Naimie, C.E. (1995a) *On the Modeling of the Seasonal Variation of the Three-Dimensional Circulation Near Georges Bank*, PhD Dissertation, Dartmouth College, Hanover, New Hampshire, 266pp.

Naimie, C.E. (1995b) Georges Bank residual circulation during weak and strong stratification periods - prognostic numerical model results. Submitted.

Owen, R.W. (1989) Microscale and finescale variations of small plankton in coastal and pelagic environments. *J. Mar. Res.*, **47**, 197-240.

Page, F.H., and K.T. Frank (1989) Spawning time and egg-stage duration in Northwest Atlantic haddock (*Melanogrammus aeglefinus*) stocks with emphasis on Georges and Browns Bank. *Can. J. Fics. Aquat. Sci.*, **46**(Suppl. 1), 68-81.

Rothschild, B.J. (1992) Application of stochastic geometry to problems in plankton ecology. *Phil. Trans. R. Soc. Lond.*, **B336**, 225-237.

Rothschild, B.J. and T.R. Osborn (1988) Small-scale turbulence and plankton contact rates. *J. Plankton Res.*, **10**, 465-474.

Sundby, S. and P. Fossum (1990) Feeding conditions of Arcto-Norwegian cod larvae compared with the Rothschild and Osborn theory on small-scale turbulence and plankton contact rates. *J. Plankton Res.*, **12**, 1153-1162.

Thomson, D.J. (1987) Criteria for the selection of stochastic models of particle trajectories in turbulent flows. *J. Fluid Mech.*, **180**, 529-556.

Werner, F.E., F.H. Page, D.R. Lynch, J.W. Loder, R.G. Lough, R.I. Perry, D.A. Greenberg, and M.M. Sinclair (1993) Influences of mean advection and simple behavior on the distribution of cod and haddock early life stages on Georges Bank. *Fish. Oceanogr.*, **2**, 43-64.

Werner, F.E., R.I. Perry, R.G. Lough and C.E. Naimie (1995) Trophodynamic and Advective Influences on Georges Bank Larval Cod and Haddock. *Deep Sea Research II*, in press.

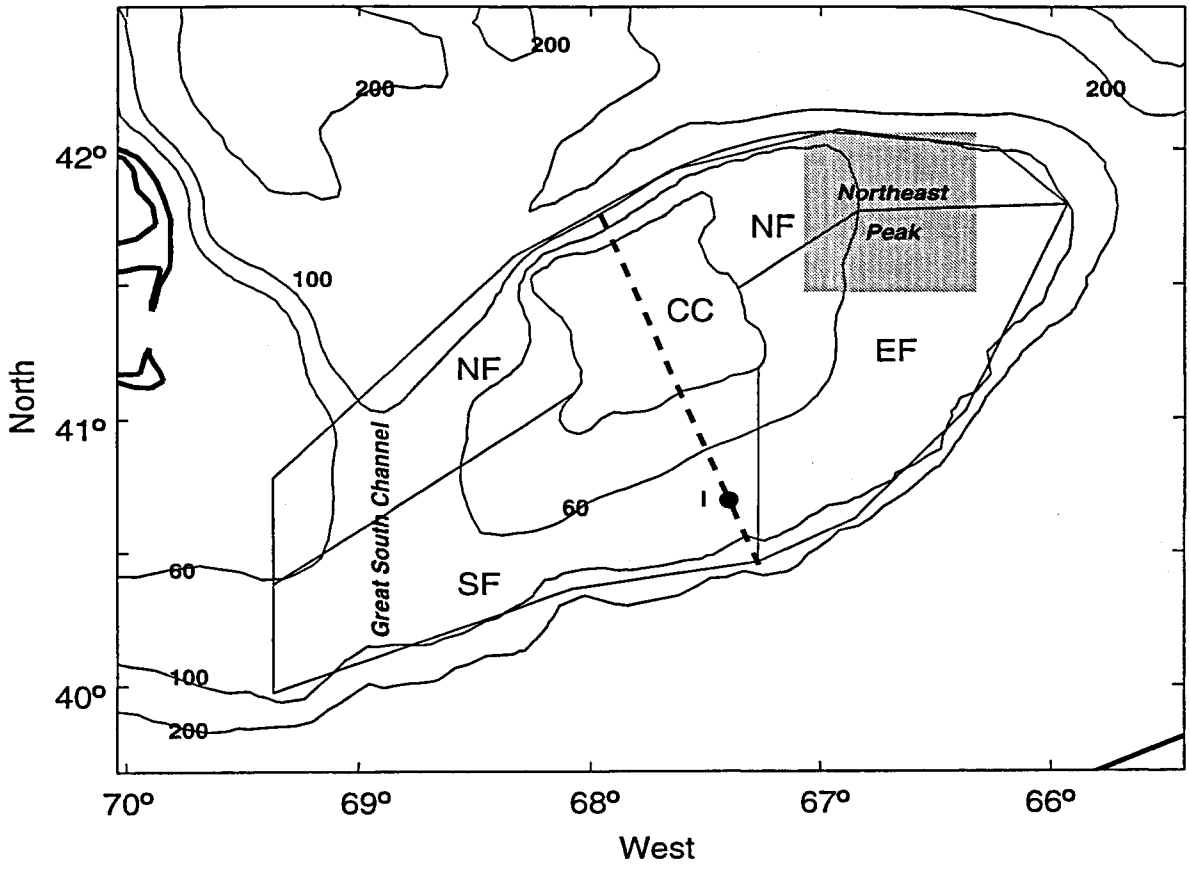

Figure 1: Georges Bank bathymetry (m) and prey field sectors. The northern flank (NF), the eastern flank (EF), the southern flank (SF) and central cap (CC) prey regions/sectors are outlined; the spawning grounds, located on the Northeast Peak, are indicated by the shaded square. The outline of the Central Cap is defined by the 40 m isobath. The dashed line indicates the section along which values of turbulent kinetic energy dissipation are shown in Figure 3. A time-history and vertical profile of the turbulent kinetic energy dissipation ϵ is at Site I is shown in Figures 3.

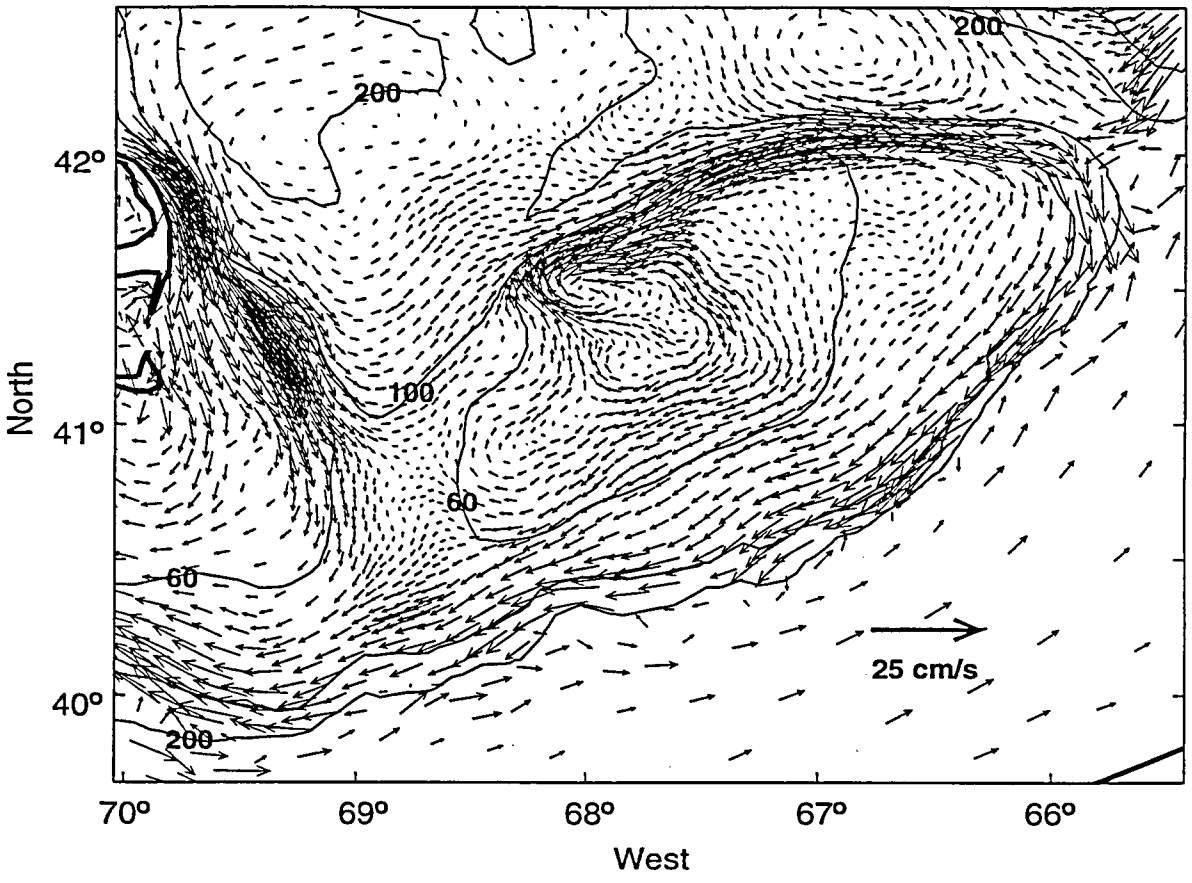

Figure 2: Depth-averaged residual flow field.

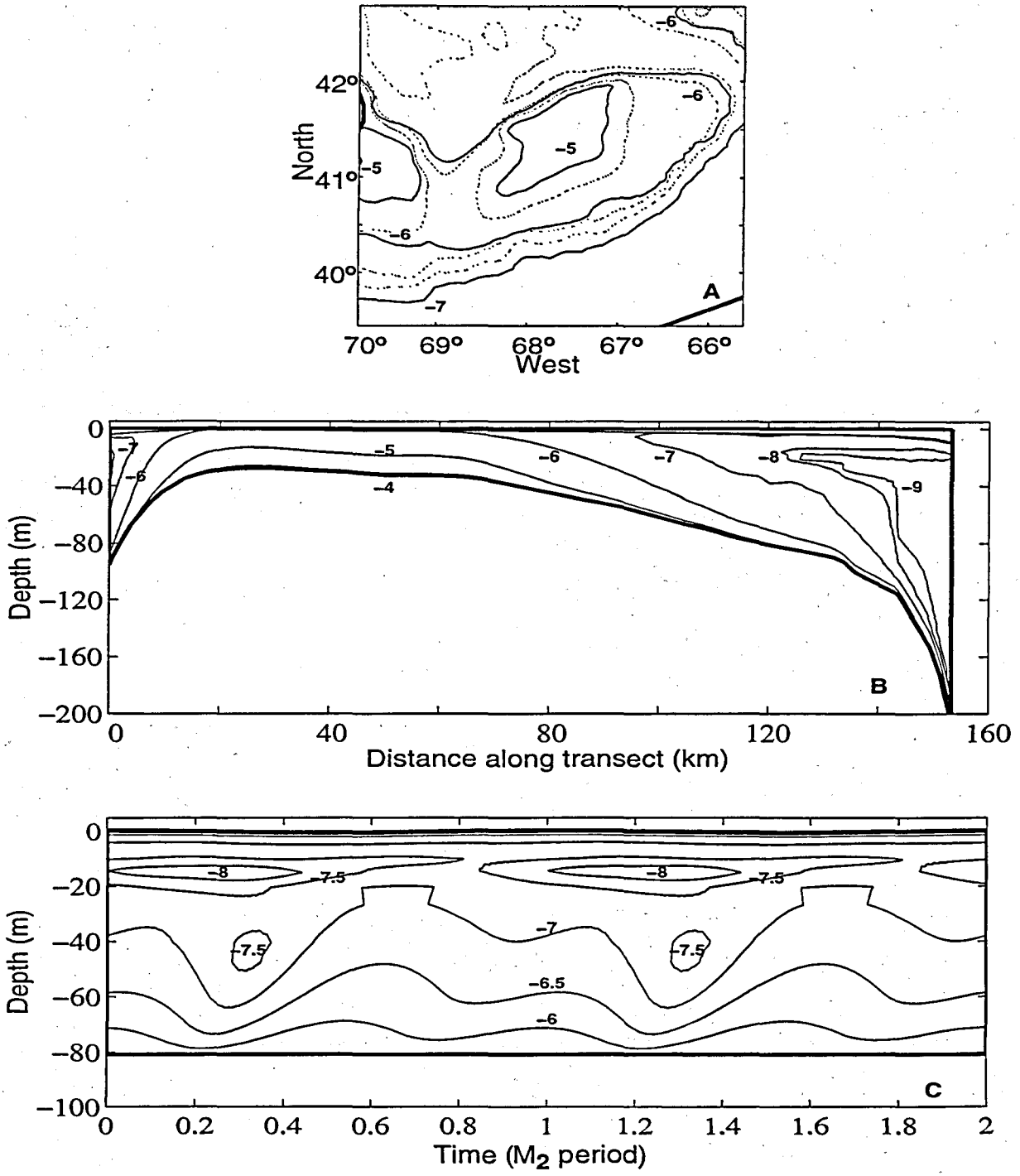

Figure 3: Top panel (A): depth-averaged turbulent kinetic energy dissipation rate $\bar{\epsilon}$ (W/Kg) at a point in time during the M_2 tidal cycle (isobaths indicates by dotted lines); middle panel (B): vertical section of ϵ (W/Kg) across the Bank from northern (NF) to southern flank (SF), along the transect indicated in Figure (1) and point in time as in (A); bottom panel (C): vertical profile of the turbulent kinetic energy dissipation rate ϵ (W/Kg) over two tidal cycles at Site I (Fig. 1) on the southern flank (the time series was reconstructed using the residual, M_2 and M_4 components).

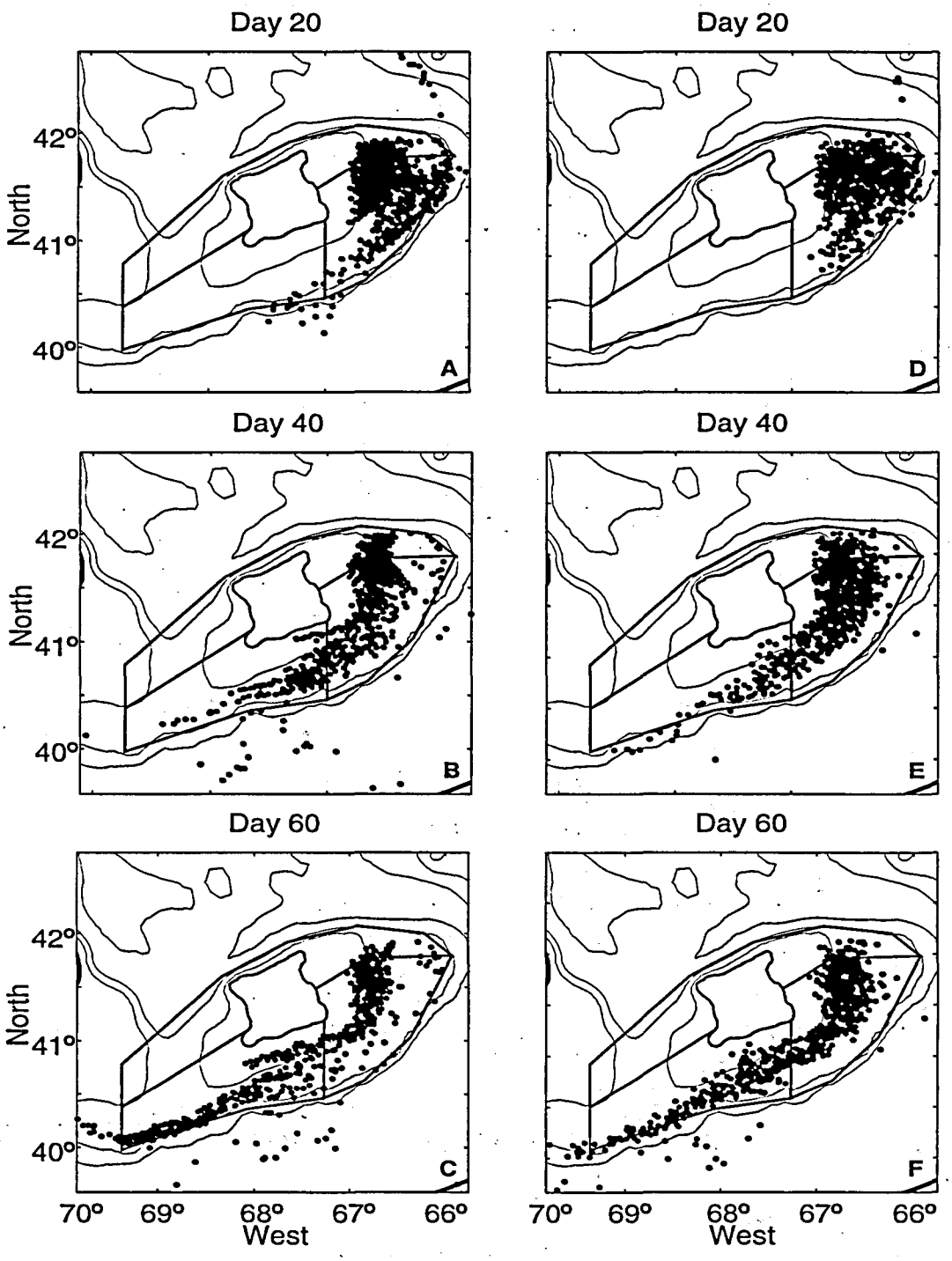

Figure 4: Particle locations on Georges Bank at hatch (day 20 post-spawn), 40 days post-spawn, and 60 days post-spawn. The trajectories shown in the three left-most panels (A, B and C) were computed using the time-dependent, non-turbulent velocity field. The trajectories shown in the three right-most panels (D, E and F) were computed including the effect of turbulent "kicks" in the vertical (see Section 7). Isobaths and regions as in Figure 1.

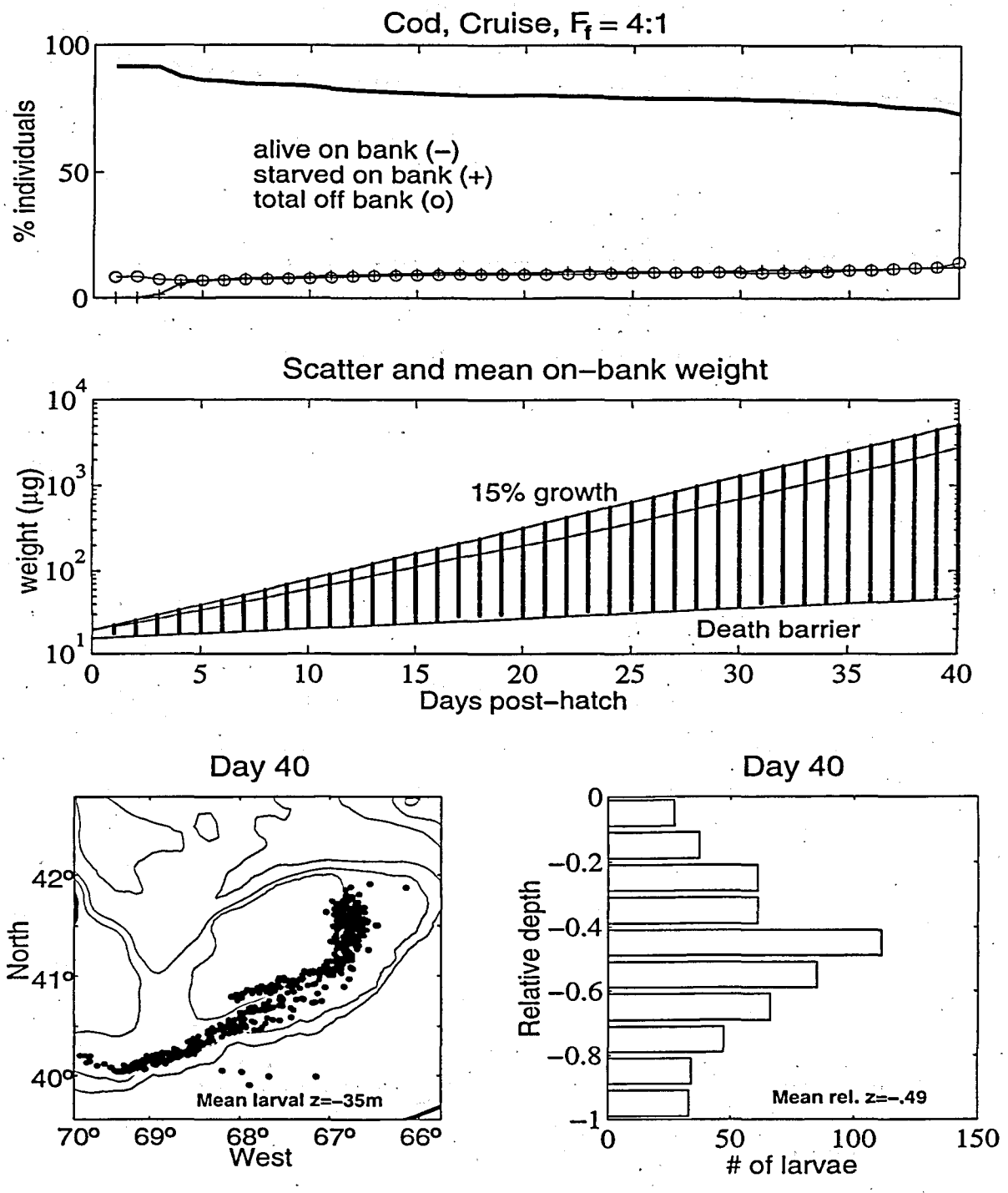

Figure 5: Post-hatch time history of cod larvae with cruise behavior and F_f=4:1. Top left panel, the percentage of larvae alive (solid line), starved on-Bank (solid line with crosses), and advected off the Bank (solid line with open circles); top right panel, the daily size distribution (μg) for the live larvae on the Bank, the 15% per day growth curve, the death barrier and the mean daily weight of those live larvae still on the Bank. Also shown are the horizontal distribution of the live larvae (bottom left panel) and their vertical distribution relative to the local bottom-depth (bottom right panel).

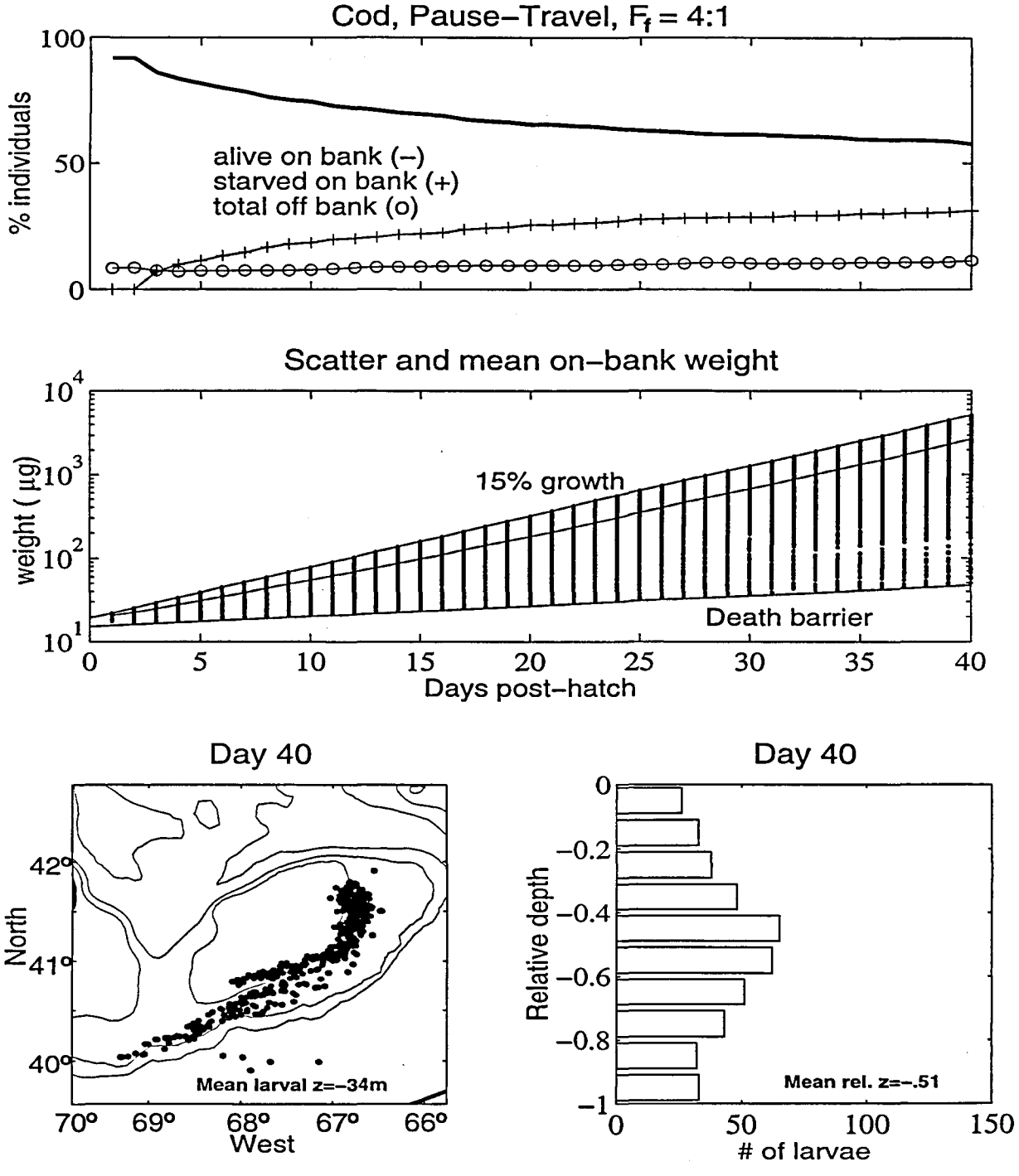

Figure 6: As in Figure (5) except for pause-travel behavior.

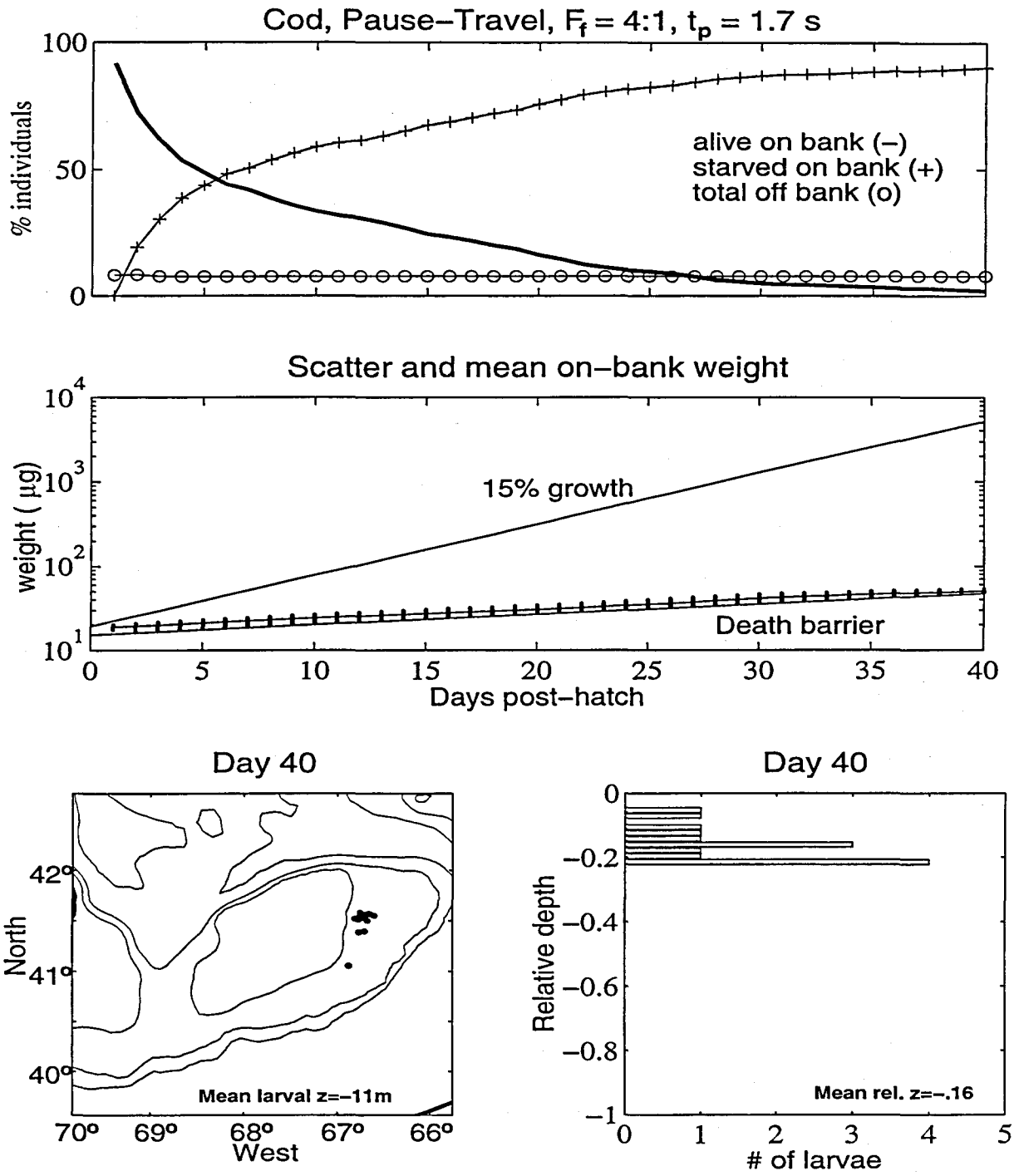

Figure 7: As in Figure (6) except for pause-travel behavior and including the effect of turbulence on the ability of larvae to pursue and capture prey that are encountered. The pursuit time t_p was set at 1.7 sec.

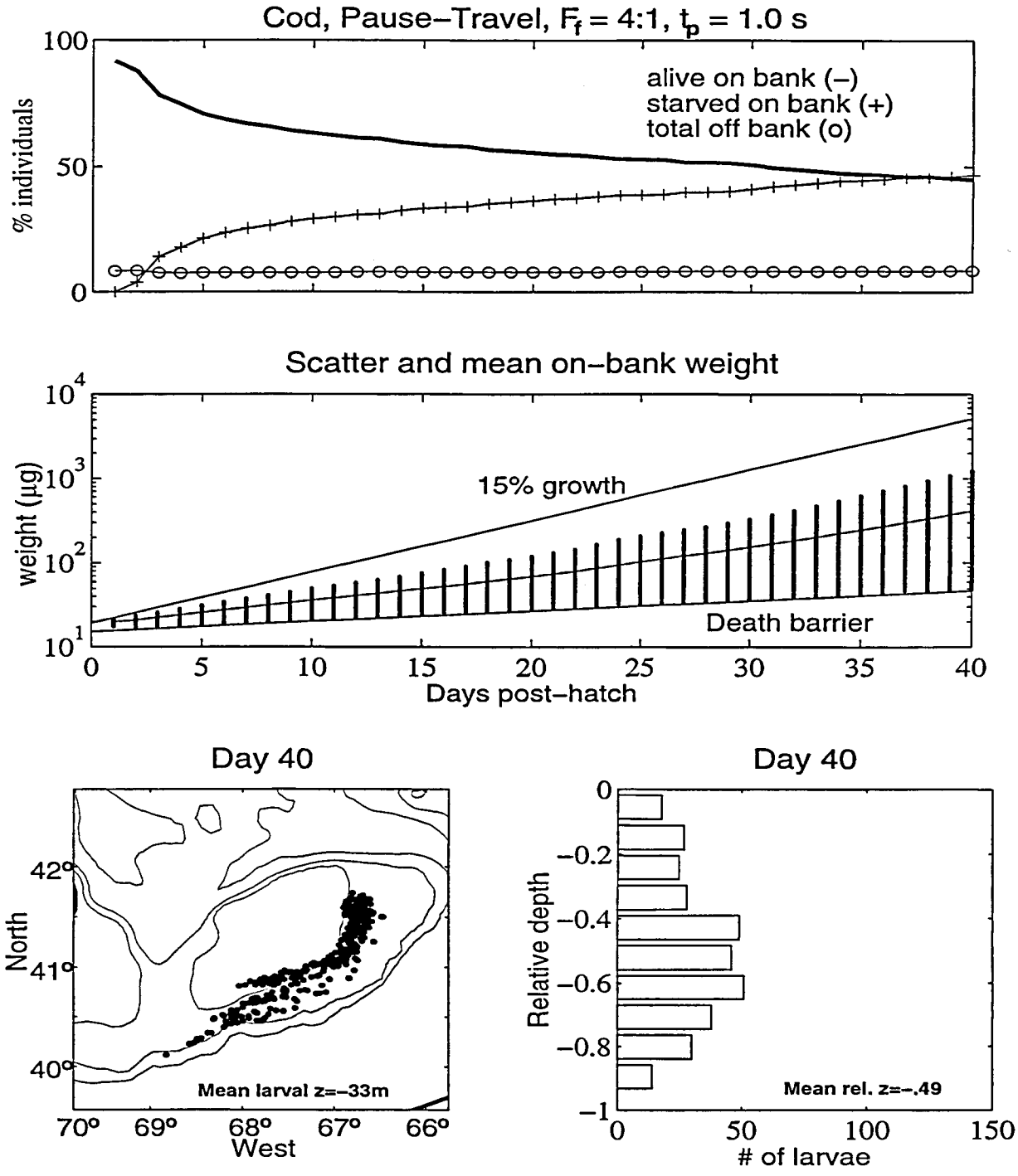

Figure 8: As in Figure (7) except for the pursuit time t_p which was set to 1.0 sec.

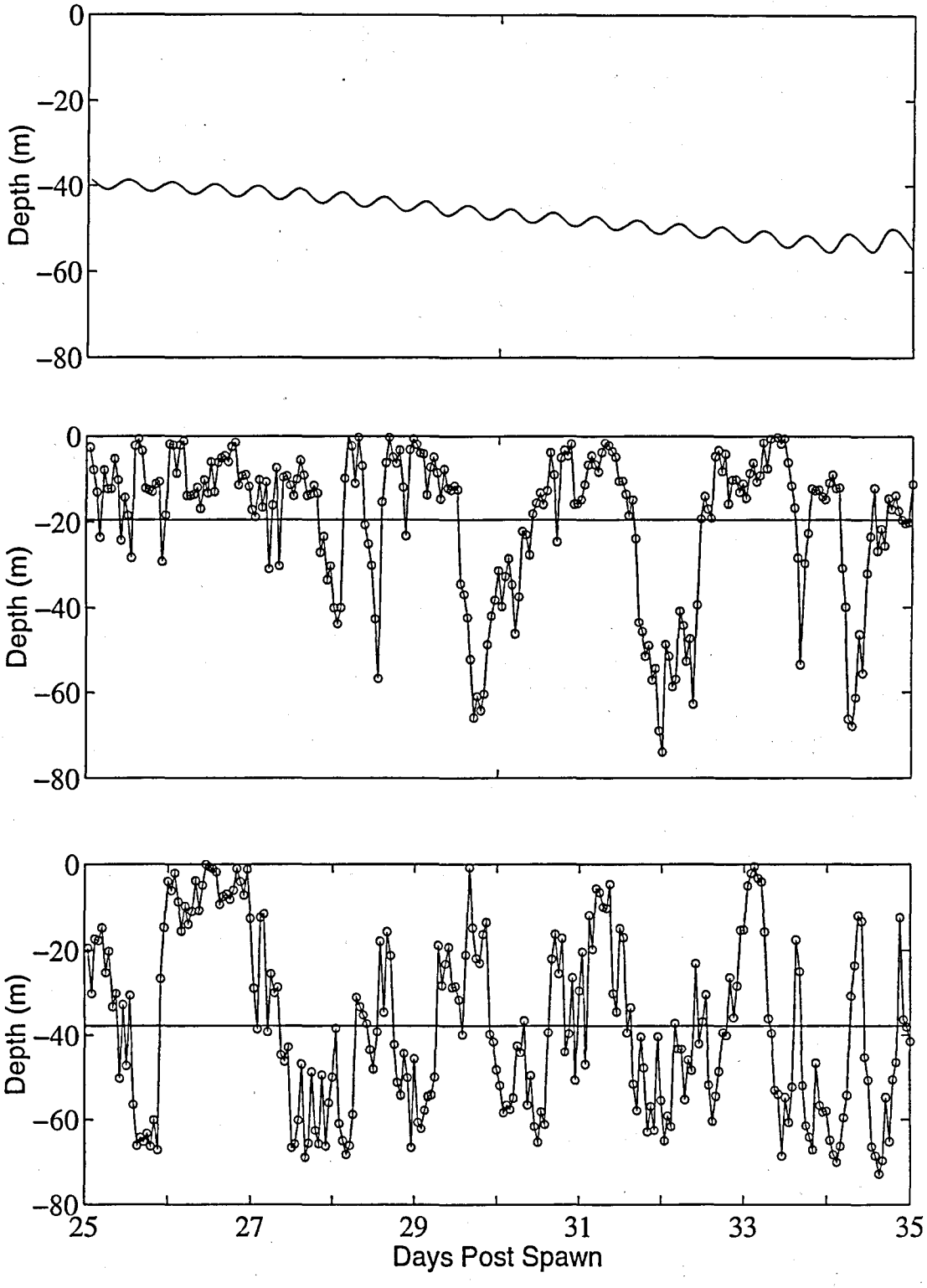

Figure 9: Time-history of hourly vertical positions during days 25-35 post-spawn for larva #350. Top panel: without turbulent "kicks"; middle panel: with the inclusion of vertical "kicks" without the term F in Eq. (10); and bottom panel: with the inclusion of vertical turbulent "kicks" as in Eq. (10). The horizontal lines in the middle and bottom panels indicate the mean depth over the 10-day time period.

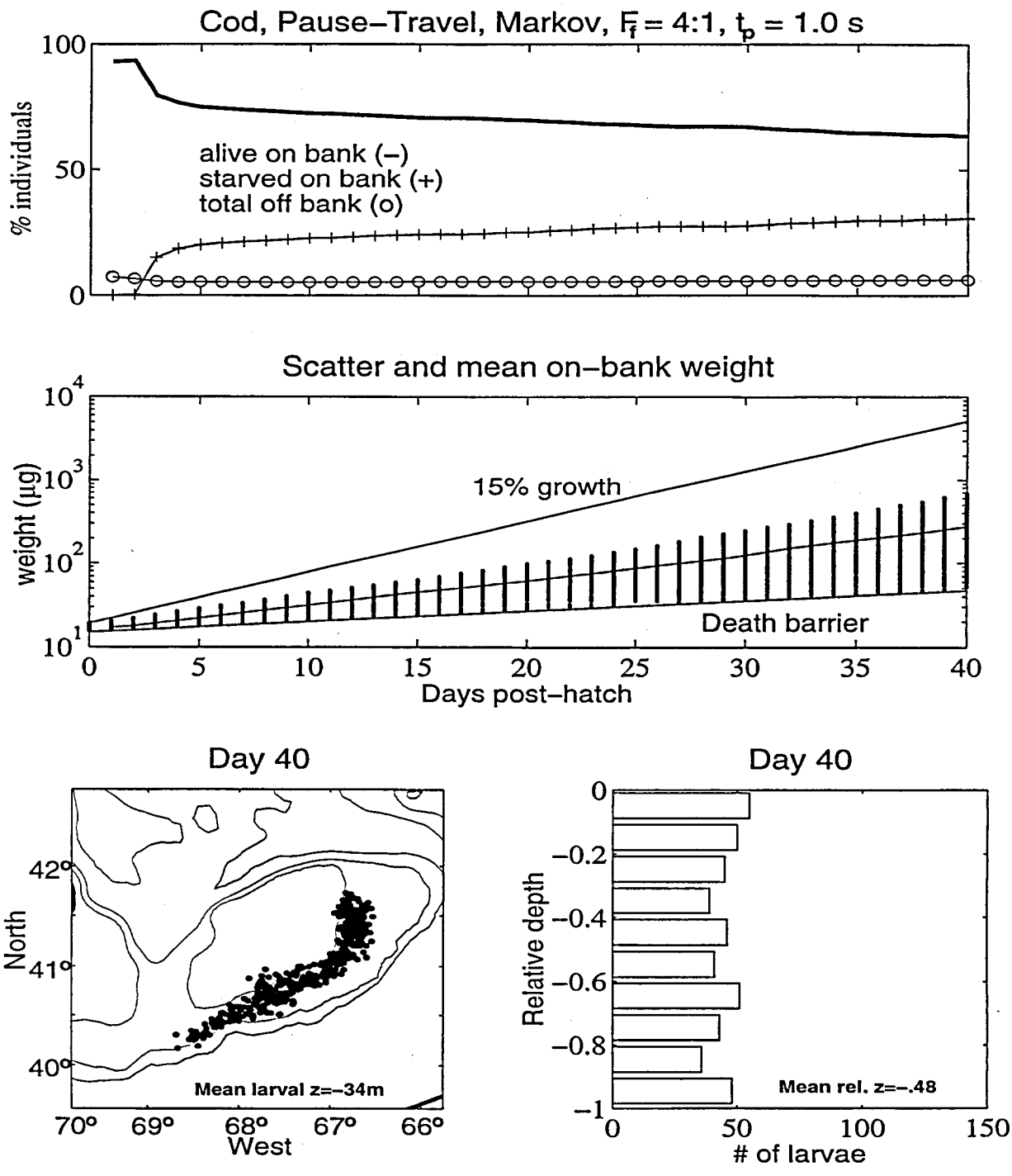

Figure 10: As in Figure (8) but with the inclusion of vertical turbulent "kicks".